UCRL 568
Copy 2

# UNIVERSITY OF CALIFORNIA

# Radiation Laboratory

TWO-WEEK LOAN COPY

*This is a Library Circulating Copy which may be borrowed for two weeks. For a personal retention copy, call Tech. Info. Division, Ext. 5545*

BERKELEY, CALIFORNIA

## DISCLAIMER

This document was prepared as an account of work sponsored by the United States Government. While this document is believed to contain correct information, neither the United States Government nor any agency thereof, nor the Regents of the University of California, nor any of their employees, makes any warranty, express or implied, or assumes any legal responsibility for the accuracy, completeness, or usefulness of any information, apparatus, product, or process disclosed, or represents that its use would not infringe privately owned rights. Reference herein to any specific commercial product, process, or service by its trade name, trademark, manufacturer, or otherwise, does not necessarily constitute or imply its endorsement, recommendation, or favoring by the United States Government or any agency thereof, or the Regents of the University of California. The views and opinions of authors expressed herein do not necessarily state or reflect those of the United States Government or any agency thereof or the Regents of the University of California.

UNIVERSITY OF CALIFORNIA
RADIATION LABORATORY

Cover Sheet
Do not remove

INDEX NO. UCRL 568
This document contains ___ pages
and ___ plates of figures.
This is copy 2 of ___. Series ___

Issued to:

INFORMATION DIVISION
RADIATION LABORATORY
UNIVERSITY OF CALIFORNIA
BERKELEY, CALIFORNIA

**UNCLASSIFIED**

Classification

Each person who received this document must sign the cover sheet in the space below.

| Route to | Noted by | Date | Route to | Noted by | Date |
|---|---|---|---|---|---|
| E. Gardner | E.G. | 2-6-50 | | | |
| H. Bradner | HB | | | | |
| J. Vale | J. Vale | | | | |
| | | | | | |
| | | | | | |
| | | | | | |
| | | | | | |
| | | | | | |
| | | | | | |
| | | | | | |
| | | | | | |
| | | | | | |
| | | | | | |
| | | | | | |

R-41

COPY 2
UCRL 568

UNCLASSIFIED

# Production of $\pi$-Mesons in Lead by High Energy Proton Bombardment

By

Mitchel Weissbluth
A.B. (Brooklyn College) 1936
M.A. (George Washington University) 1941

DISSERTATION

Submitted in partial satisfaction of the requirements for the degree of

DOCTOR OF PHILOSOPHY

in

Physics

in the

GRADUATE DIVISION

of the

UNIVERSITY OF CALIFORNIA

Approved:

. . . . . .

. . . . . .

. . . . . .

Committee in Charge

Deposited in the University Library . . . . . .
Date Librarian

OUTLINE

I Introduction

II Experimental Arrangement

III Classification of Mesons

IV Calculation of the Cross Section

V Corrections

1. Decay in flight
2. Extended source
3. Effective thickness of emulsion
4. Proton energy loss in the target
5. Meson energy loss in the target
6. Nuclear absorption and scattering
7. Mesons produced in absorbers
8. Small angle scattering

VI Calculations and Results

VII The Wentzel Experiment

VIII Acknowledgments

IX References

# I INTRODUCTION

Our knowledge of the properties of mesons and their interactions with nuclei has come from two sources. Studies of cosmic ray phenomena provided the earliest information. The discovery that mesons may be produced artificially[1] by bombardment of nuclei with radiations from high energy accelerators has, on the other hand, made it feasible to undertake a wide variety of investigations under more controlled conditions than is possible in cosmic ray experiments. In such experiments mesons have been produced by high-energy protons, alpha-particles and neutrons.[2] More recently, mesons have been produced by high-energy x-rays[3] from the Berkeley synchrotron.

Existing information on mesons establishes certain of their basic properties, in particular, the mass[4,5] and charge[6] of the $\pi$ and $\mu$ meson, their respective half-lives[7,8] and the fact that $\pi$ mesons interact strongly with nuclei.[9] The latter is borne out by the observation that $\pi$'s are produced in nucleon-nucleon encounters, and that negative $\pi$'s usually produce nuclear stars when they are brought to rest. Further information on the nature of the interaction between mesons and nuclei can be obtained from experiments in which the scattering, capture, or production of mesons are observed. Scattering and capture experiments are considerably more difficult than production experiments. Furthermore, some knowledge of the production cross sections is essential in order to arrange a set of optimum conditions for a capture or a scattering experiment. Thus it seems reasonable that the production of mesons be studied first. Aside from their value in subsequent experiments, the production cross sections in themselves may throw considerable

light on the nature of the interaction between mesons and nuclei.

In arranging an experiment on the production of mesons, it is desirable that the nucleus in which the mesons are produced be of a simple type such as hydrogen or deuterium, so that the results will not be affected by features which depend upon unkown or unanalyzable details of nuclear structure. On the other hand, materials containing heavier nuclei are much more convenient to handle experimentally. Experiments with heavier nuclei establish the general order of magnitude of meson production cross sections and they give information regarding successful experimental techniques which is of considerable value in arranging the more fundamental experiments involving hydrogen or deuterium.

The techniques for the study of the production and properties of mesons artificially produced by the high energy synchro-cyclotron at the University of California Radiation Laboratory have generally made use of the internal beam circulating in the vacuum tank of the cyclotron, where the high particle flux and the presence of the cyclotron's magnetic field have been used to great advantage in numerous experiments.[2] An increase in the scope of possible experiments, and a greater flexibility both in the detection of mesons and in the monitoring of the cyclotron beam resulted when Richman and Wilcox[10] devised a technique which enabled them to perform meson experiments in the deflected external beam of the cyclotron. This technique was used in the work to be described.

The cross section for the production of $\pi$ mesons in carbon by 345 Mev protons was measured by Peterson[11] for mesons with energies of

11-13 Mev and which were emitted at angles $0^{\circ}$-$30^{\circ}$ to the direction of the proton beam. A comprehensive investigation of the production of both positive and negative $\pi$ mesons in carbon by protons was in progress by Richman and Wilcox at the time this experiment was undertaken. With regard to the production of mesons in heavy elements, however, very little information was in existence. It was therefore the object of the present investigation to determine the characteristics of meson production in a heavy nucleus such as lead, and to compare the results with those obtained in the light nucleus, carbon.

The technique of Richman and wilcox[10] lends itself easily to a determination of absolute cross sections for the production of both positive and negative mesons over the entire spectrum. The mesons are detected in nuclear emulsions and in spite of a considerable number of background tracks, meson tracks have a sufficient number of distinguishing characteristics to be easily recognized. The energies of the mesons are determined by their ranges in aluminum and copper.

$\pi$ mesons emitted from lead at $90^{\circ}$ to the direction of the 345 Mev proton beam are distributed over a range of 0-120 Mev for positives and 0-90 Mev for negatives. A peak at about 40 Mev occures in the positive spectrum with a differential cross section of $(11.8 \pm 2) \times 10^{-30}$ $cm^2$ $(Mev)^{-1}$ $(steradian)^{-1}$ $(lead\ nucleus)^{-1}$; the spectrum of negative mesons has a maximum at about 30 Mev where the cross section is $(11.5 \pm 2.3) \times 10^{-30}$ $cm^2$ $(Mev)^{-1}$ $(steradian)^{-1}$ $(lead\ nucleus)^{-1}$. At low meson energies, about 18 Mev, the ratio of negative to positive $\pi$ mesons is approximately unity; at higher energies, the ratio becomes smaller and approaches zero at about 90 Mev.

A further study was made of the angular distribution of the $\mu$ mesons in $\pi$-$\mu$ decay. The distribution was found to be isotropic. This result is discussed in the light of Wentzel's suggestion[12] of the relationship between the angular distribution of the $\mu$ mesons and the spin of the $\pi$ mesons.

## II EXPERIMENTAL ARRANGEMENT

A schematic diagram of the experimental arrangement is shown in Fig. II-1. The deflected proton beam from the cyclotron passes through a slit, through a steering magnet and finally emerges outside of the main concrete shielding around the cyclotron. A tube, set in the concrete shielding through which the beam passes, is of such size and is so aligned that the protons pass through it without striking the walls. Thus, the emerging beam is essentially free of scattered particles. The beam energy is 345 $\pm$ 1 Mev. The cross-sectional area of the beam may be adjusted by varying the slit dimensions; however, a compromise must be sought between maximum current and good geometrical definition of the beam at the traget. For this experiment the cross section of the beam was approximately a 1 1/4 x 1 1/4 inch square, with an average current of 3-5 x $10^{-11}$ amperes.

As shown in Fig. II-1, the beam, after traversing the target, is caught in a Faraday cup* of sufficient thickness completely to stop all protons. The charge collected by the Faraday cup is accumulated on a condenser whose voltage increase is carefully measured at convenient intervals. Thus the number of protons bombarding the target is known to an accuracy of about $\pm$ 3 percent and it becomes possible to calculate cross sections on an absolute scale. The fact that the external beam may be accurately and conveniently integrated represents an advantage over techniques which make use of the internal circulating

---

*The Faraday cup and associated circuits were kindly made available by V. Z. Peterson.

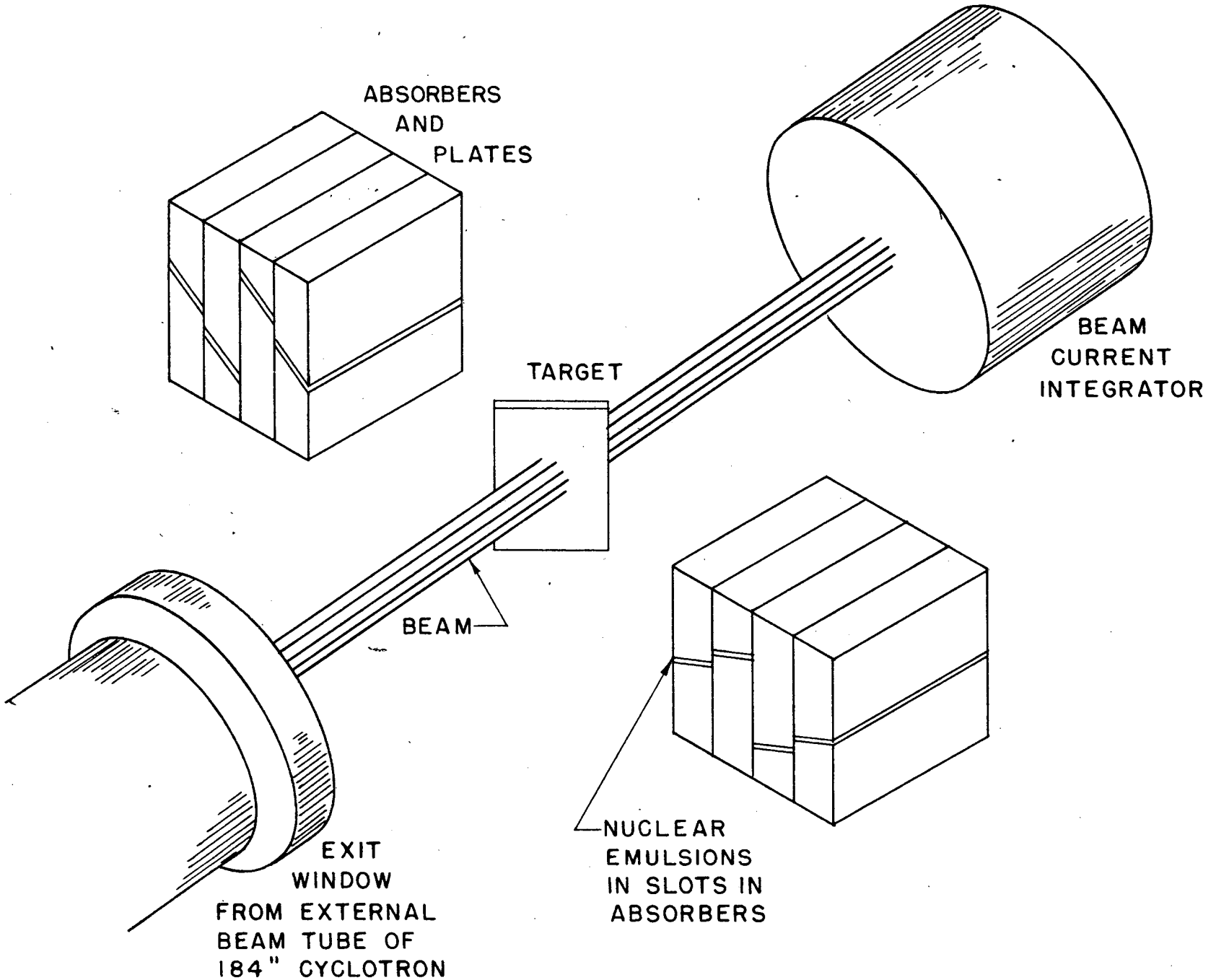


FIG. II-1

14404-1

beam inside the cyclotron vacuum tank where the integration of the beam can only be accomplished by indirect methods.[1]

A rectangular lead target 3 x 5 inches was inclined at 45° to the beam. For the detection of mesons of low energy, up to about 45 Mev, a target thickness of 0.050 inch was used. For higher energy mesons, the target thickness was increased to 0.250 inch. The lead was of normal isotopic composition.

Sets of absorbers are placed on either side of the beam as shown in Fig. II-1. The absorbers contain photographic plates inclined at 15° to the horizontal and placed in position to accept particles emanating from the target at a mean angle of 90° to the beam direction. The departure from 90° was no greater than ± 7° for any region scanned. The identification of mesons will be discussed in detail in Section III; for the present it is only necessary to note the meson tracks are observed in the close neighborhood of their ends. Consequently the position of a meson on the photographic plate reveals its energy, since it had to traverse a certain thickness of absorber material to reach the particular point on the photographic plate. Thus, the complete meson energy spectrum is obtained.

The absorbers in which the mesons lose their energy are 3 x 3 1/2 x 0.982 inches, with a 15° cut to hold the photographic plate (Fig. II-2). A piece of black masking tape around the cut keeps the plate from being light-struck. The absorber block nearest the target is at a distance of 7.15 cm from the center of the target. It is made of aluminum and is capable of stopping mesons from 0-37 Mev. The next absorber, placed immediately behind the first is made of copper

and is capable of stopping mesons from 37-85 Mev; the third absorber covers the range 85-125 Mev. In this way, as many absorbers as may be necessary to cover the entire meson spectrum are placed one behind the other. As will be shown later, the meson spectrum effectively ends at about 120 Mev; thus, three absorbers are required.

The absorber nearest the target is made of aluminum in order to expand the low energy portion of the meson spectrum over a larger area of the photographic plate. On the other hand, the use of aluminum for all of the absorbers would materially reduce the effective solid angle subtended by a given area of the plate at the target for the higher meson energies, so the subsequent absorbers are made of Cu. The absorbers were large enough so that most of the area of the photographic plate was essentially surrounded by an infinite sea of absorber medium. Thus, except near the extreme edges there is no significant loss of particles from the absorber through small angle scattering.

The photographic plates used in this experiment were Ilford C-3 100-micron plates. These plates are sufficiently sensitive so that the entire track of a $\mu$ meson originating from the decay of a $\pi$ meson in the emulsion is easily recognized, yet the plates are not so sensitive as to obliterate the characteristic increase in ionization when a meson approaches the end of its range. Electrons are not observed in this type of emulsion.

In principle, it would be desirable to expose the photographic plates for such a long time that the density of mesons on the plate is sufficiently high for rapid counting. This situation does not

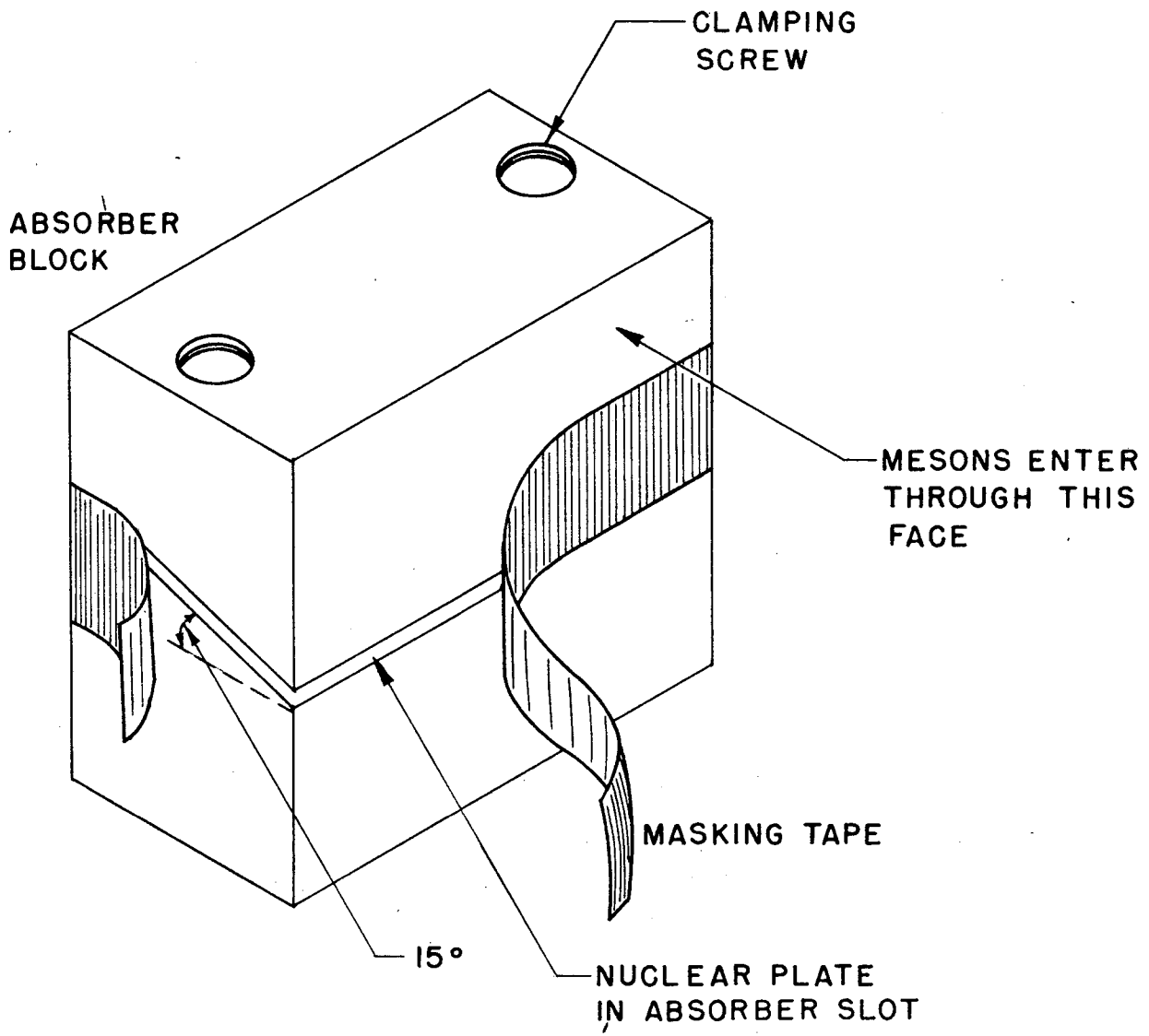


FIG. II - 2

14403-1

exist in practice, however. The cross section for scattered protons is of the order of 1000 times larger than the cross section for producing mesons. Hence the duration of the exposure necessary to produce a plate such that a meson can be reliably recognized and identified amidst other tracks is entirely controlled by the background radiation.

Background radiation which directly or through a chain of reactions leads to charged particles capable of producing tracks in the emulsion, comes principally from three sources - the target, the integrator in which the beam is stopped, and the cyclotron. Lead shielding around the absorbers which hold the photographic plates (not shown in Fig. II-1) helps to reduce the background from the latter two sources. Background radiation from the target is unavoidable in the present arrangement

There is a qualitative difference in the appearance of a plate placed in a position to record low energy mesons from one which records high energy mesons. The preferred orientation of the background tracks in the low energy plates shows that the predominant low energy charged particle background originates at the target. The spectrum of the charged particle background and also the solid angle per unit area rapidly falls as the distance from the target increases, so it was found to be desirable to use three different low energy plates, exposed consecutively in the same location for three different time intervals, in order to have an approximately optimum exposure in each of the energy regions covered by the plate. On the other hand, the plates exposed in a position to record high energy mesons show

background tracks oriented in all directions - an indication that here the charged particle background is of a random nature, that is, the particles do not come directly from the target. These charged particles are produced by the ambient neutron flux. Thus, the time required to obtain a plate with a given number of background tracks approaches a value which is only slowly varying with the distance from the plate to the target.

## III CLASSIFICATION OF MESONS

Bombardment of nuclei with high energy particles (or photons) results in the emission of positive and negative $\pi$ mesons. Some evidence for the production of neutral mesons[1] has also been reported. Neutral mesons are not observable in this experiment. In spite of the absence of a magnetic field to provide a charge separation, it is nevertheless possible in this experiment to distinguish positive from negative mesons because of the following considerations: A positive $\pi$ meson which comes to the end of its range always decays into a positive $\mu$ meson[2] and another light neutral particle which is presumably a neutrino. The positive $\mu$ meson, originating from a stopped $\pi^+$ meson is monoenergetic with an energy of $4.18 \pm 0.04$ Mev.[3] Negative mesons generally produce nuclear stars. It has been found from studies[4] on the prong distribution of stars from magnetically sorted mesons that $73 \pm 2$ percent of the negative $\pi$'s produce a nuclear star of one or more observable prongs. The remaining 27 percent of the $\pi^-$ mesons end in the emulsion without initiating an observable event, presumably emitting neutrons. Thus it is seen that positive and negative $\pi$ mesons have characteristics which render them distinguishable even when appearing together in an emulsion.

We now consider a more detailed classification based on the actual appearance of mesons in the emulsion:

1. A meson ends in a star of two or more prongs. This is identified as a negative $\pi$ meson and is given the classification $\pi^*(2,3,\ldots)$. No stars have been observed from $\pi^+$, $\mu^+$ or $\mu^-$ mesons.[5] The case of one-prong stars will be considered separately.

2. A meson ends with the subsequent emission of another meson. The secondary meson is identified as such by virtue of the characteristic wandering due to small angle scattering and a rapid increase in grain density near the end of the range. Furthermore, the track is about 615 microns[6] long which is the range in emulsion of a $\mu$ meson originating from a stopped meson. This is then a $\pi$-$\mu$ decay. $\pi^-$ mesons, when stopped in matter, have never been observed to decay into $\mu^-$ mesons in some 4000 tracks that have been studied.[6] In vacuum, a $\pi^-$ meson will decay into a $\mu^-$ meson and a neutrino. A $\pi$-$\mu$ decay is therefore counted as a positive $\pi$ meson.
3. Mesons appear in the emulsion which stop with no observable subsequent event. Such a meson, designated as a $\rho$ meson, may be one of the following types:
   a) It may be a $\mu^+$ meson originating from a $\pi^+$ meson which has come to rest in the glass or absorber surrounding the emulsion. Such a meson, even if definitely identified as a $\mu^+$, is indicative of a $\pi^+$ outside of the specified volume of emulsion which is used in computing the cross section. It is therefore not counted.
   b) It may be a negative $\pi$ meson which does not initiate a star with observable prongs. This occurs, as mentioned above, in 27 percent of the cases. Such mesons are taken into account by the correction applied to the number of definitely identified

negative $\pi$ mesons, namely

$$(1 - .27)N_{\pi^-}^{true} = N_{\pi^*}^{observed} \qquad \text{III-1}$$

or $$N_{\pi^-}^{true} = 1.37\, N_{\pi^*}^{observed}$$

c) The $\rho$ meson may be a positive or negative $\mu$ from a positive or negative $\pi$ which decayed in flight. An overall correction for decay in flight is applied and will be discussed in Section V.

4. A meson appears in the emulsion and stops; a thin, lightly ionizing, track emerges. The secondary track leaves the emulsion in a distance too short for its identity to be definitely ascertained. Such an event may arise from one of the following:

   a) A positive $\pi$ meson decays into a positive $\mu$ meson. The $\mu$ meson emerges at such an angle as to leave the emulsion before it is stopped or scatters appreciably.

   b) A negative $\pi$ meson initiates a one-prong star. The single prong is a track left by a heavy particle, (presumably a proton,) of sufficient energy to leave a lightly ionizing track whose appearance is not readily distinguishable from a track left by a $\mu$ meson. The heavy particle responsible for the prong leaves the emulsion in a distance shorter than the range of $\mu$ mesons.

It will be shown that mesons of type (4) may all be classified as

positive mesons undergoing $\pi$-$\mu$ decay.

We now consider the case of one-prong stars in some detail. Usually one-prong stars are relatively short ( $<200\ \mu$) heavily ionizing tracks whose identification is unambiguous. This is borne out by experiments[7] with magnetically separated mesons, where it was found that 73 percent of one-prong stars are of the above variety. Twenty-three percent of the one-prong stars were thin lightly ionizing tracks, but which had an unmistakable short, heavily ionizing, club-like recoil track of the order of 2-3 microns at the origin of the star. The remaining 4 percent of the one-prong stars might be confused with mesons undergoing $\pi$-$\mu$ decay. Since the one-prong stars as a group constitute 23.6 percent[4] of the total number of star-producing mesons, less than 1 percent of all the negative mesons are confusable with positive mesons. This is the justification for mesons of type (4) being classified as positive mesons undergoing $\pi$-$\mu$ decay.

## IV CALCULATION OF THE CROSS SECTION

The cross section per unit energy per unit solid angle per nucleus at an energy E and angle of emission $\theta$ is given by

$$\frac{d\sigma}{dE\,d\Omega}(E,\theta) = \frac{N_o}{nm\,\Delta E\,\Delta\Omega} \qquad \text{IV-1}$$

where

$N_o$ = number of mesons produced in the energy interval E to $E + \Delta E$ and coming off within a solid angle $\Delta\Omega$ at a particular angle $\theta$.

n = number of nuclei per $cm^2$ of the target.

m = number of incident protons.

We have

$$n = \frac{\rho t_t L}{A} \qquad \text{IV-2}$$

where

$\rho$ = density of the target in gm per $cm^3$.

$t_t$ = thickness of the target in the beam direction, in cm.

L = Avogadro's number.

A = atomic weight.

Also

$$m = \frac{Q}{e} \qquad \text{IV-3}$$

where

Q = total charge passing through the target in coul.

e = proton charge in coul.

Thus we have

$$\frac{d\sigma}{dE\,d\Omega}(E,\theta) = \frac{AeN_0}{L\rho t_t Q\,\Delta E\,\Delta\Omega}. \qquad \text{IV-4}$$

Now, $N_0/\Delta\Omega$ is the number of mesons per unit solid angle which are observed to end in a given volume of emulsion and which were originally produced with energies lying in the interval from E to E + $\Delta$E. $\Delta\Omega$ is the effective solid angle subtended by the region of emulsion in which $N_0$ mesons are observed. (Since only those mesons which stop in the emulsion are counted, $\Delta\Omega$ is not simply the projected area of the emulsion divided by the square of the distance to the target.) Suppose the average number of mesons crossing unit area of absorber and lying in the same energy interval E to E + $\Delta$E, is N. Clearly, the number of mesons per unit solid angle is then $N/\frac{1}{r^2}$. Hence

$$\frac{N_0}{\Delta\Omega} = \frac{N}{1/r^2} \qquad \text{IV-5}$$

where r is the distance to the target, temporarily considered as a point source. It is therefore necessary to find a relation between the flux N and the observed number of mesons $N_0$ in order to calculate the solid angle $\Delta\Omega$.

Let n'(E) be the flux per unit energy interval at the energy E. Since the energy may be expressed in terms of the range in a given material we can define a new function n(R) as the flux per unit range interval at range R.

Now the number of mesons that come to rest between R and R + dR is

$$n(R)dRdA$$

where dA is an element of area perpendicular to the direction of motion

of the mesons. Hence the number of stopped mesons per unit volume in an absorbing medium is just n(R).

Consider now an element of volume $dV_e$ in the emulsion (Fig. IV-1) corresponding to an increment of range $dR_a$ in the absorber.

$$dV_e = t\ell\, d\, R_a \sec \alpha \qquad \text{IV-6}$$

where t is the emulsion thickness, $\ell$ the transverse length and $\alpha$ the angle of inclination of the emulsion to the meson beam. The number of mesons coming to rest in $dV_e$ is

$$dN_o = t\,\ell \sec \alpha\, n(R_e) d\, R_a \qquad \text{IV-7}$$

where $R_e$ is the range in emulsion.

Now, the ratio of the range of a particle in one medium to its range in a second medium is approximately a constant, independent of the energy of the particle. Hence we may write

$$R_a = K\, R_e \qquad \text{IV-8}$$

and

$$dR_a = \frac{R_a}{R_e}\, d\, R_e \qquad \text{IV-9}$$

Furthermore, the flux of mesons with energies between E and E + dE is

$$n'(E)dE = n(R_a)d\, R_a = n(R_e)d\, R_e \qquad \text{IV-10}$$

Therefore from IV-9 we have

$$n(R_a)\frac{R_a}{R_e} = n(R_e) \qquad \text{IV-11}$$

Putting IV-11 into IV-7 and integrating gives

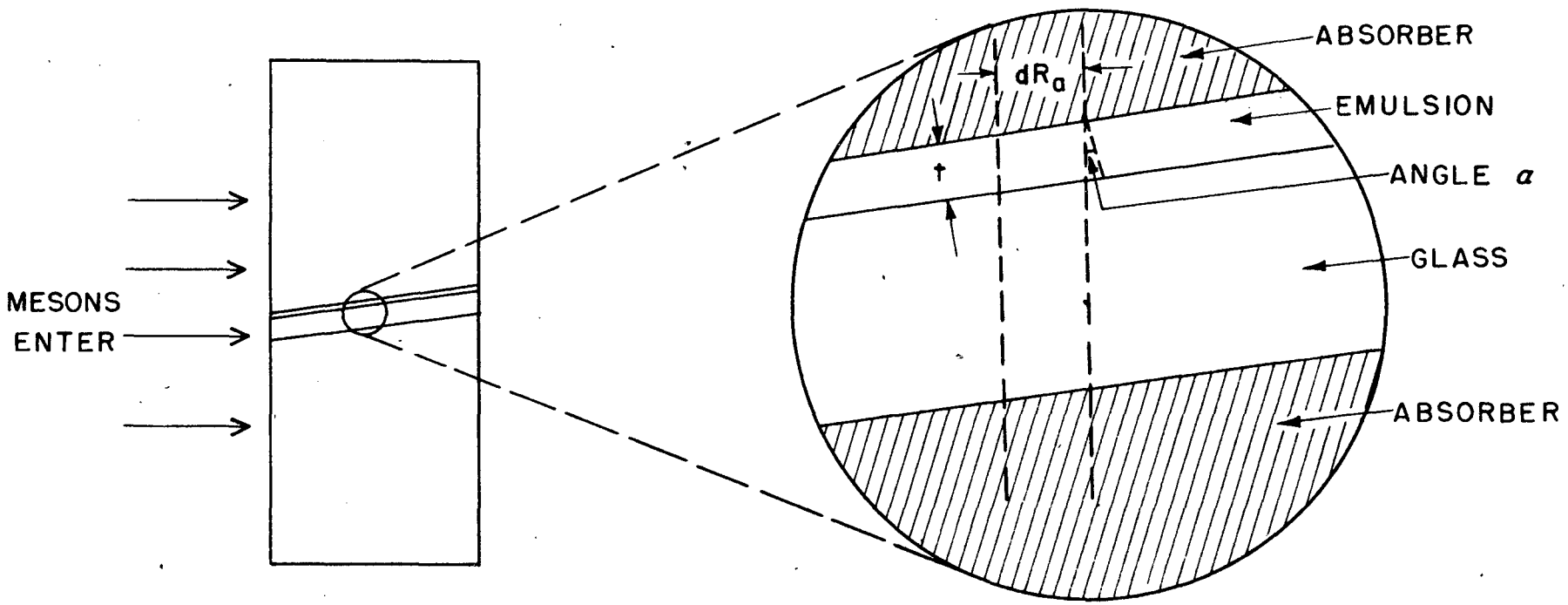


CROSS-SECTION OF ABSORBER AND EMBEDDED PHOTOGRAPHIC PLATE

ENLARGED VIEW OF PORTION OF ABSORBER AND PHOTOGRAPHIC PLATE

FIG. IV-1

$$N_o = t \frac{R_a}{R_e} \sec \alpha \, \ell \int_{R_a}^{R_a + R_a} n(R_a) d R_a$$

$$= N \ell t \frac{R_a}{R_e} \sec \alpha \qquad \text{IV-12}$$

where N is the total flux or the total number of mesons per unit area between E and E + $\Delta$E or the corresponding ranges $R_a$ and $R_a + \Delta R_a$.

Returning now to Equation IV-5 it is seen that the solid angle is given by

$$\Delta \Omega = \frac{N_o}{N} \frac{1}{r^2} = \frac{\ell t \frac{R_a}{R_e} \sec \alpha}{r^2} \qquad \text{IV-13}$$

and the formula for the cross section IV-4 becomes

$$\frac{d\sigma}{dE d\Omega}(E,\theta) = \frac{A e N_o r^2}{L \rho t_t Q \ell t \frac{R_a}{R_e} \sec \alpha \, \Delta E} \qquad \text{IV-14}$$

With the exception of t, the emulsion thickness, all of the quantities in the above expression are easily obtained or directly measured. Various corrections will be discussed in Section V.

We now consider the measurement of the emulsion thickness.

Ordinary photographic plates (obtained commercially) which are used for nuclear research may vary in thickness by as much as 25 percent. Furthermore, after development the emulsions shrink by a factor of approximately 2. Clearly it is desirable to devise some method to measure with good accuracy the actual emulsion thickness prior to development. Such a method was originated by Wilcox and used in this experiment.

The technique is illustrated in Fig. IV-2. 380 Mev alpha-particles from the cyclotron traverse the emulsion at an accurately known angle $\theta$. Such particles ionize sufficiently to leave a latent image which upon later development becomes a clearly visible track in the emulsion. This

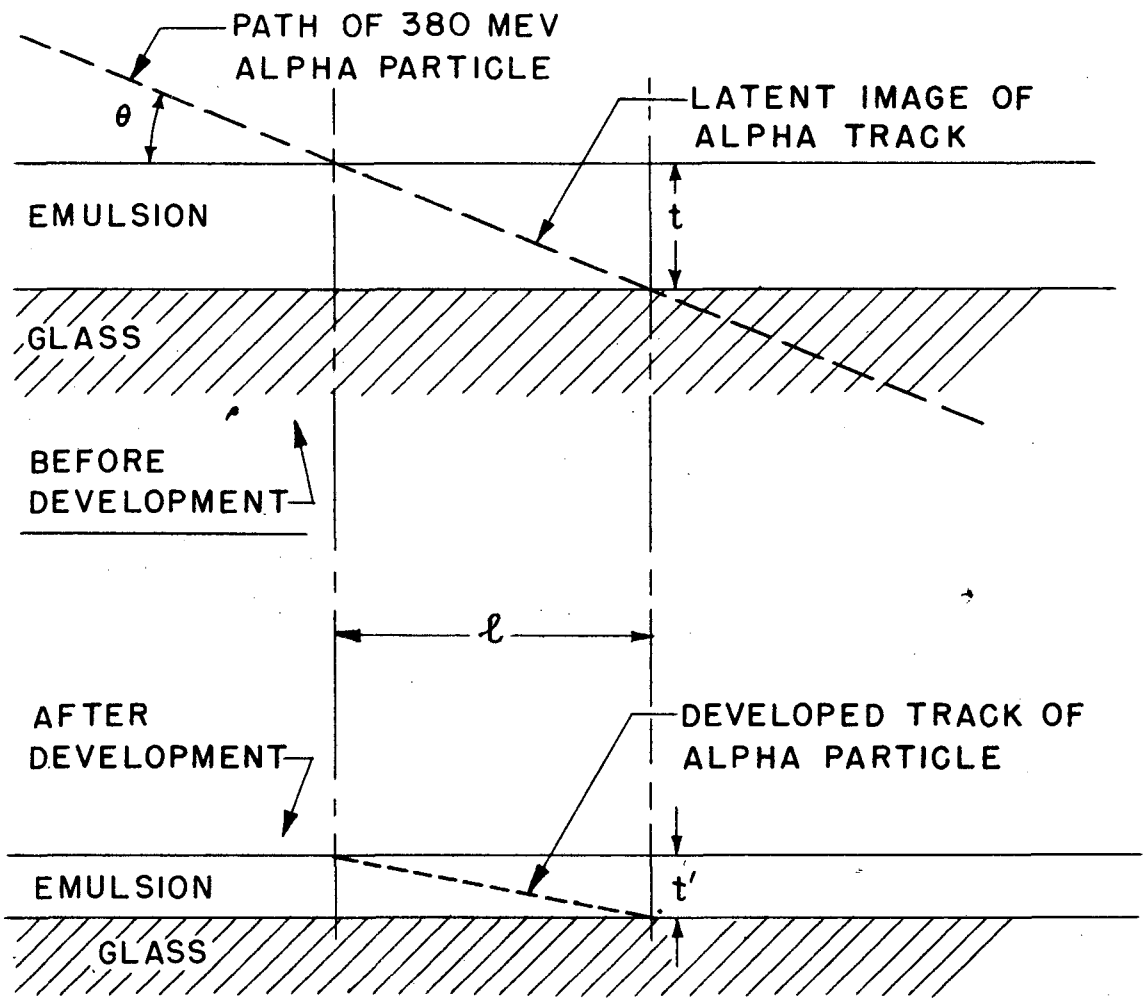


FIG. IV - 2

14405-1

latent image has a projected length $\ell$. Variations in $\theta$ arising from small angle scattering were calculated, and have been found to be negligible. Upon development, the emulsion shrinks from t to $t'$. Since one face of the emulsion is securely attached to a glass backing, $\ell$ remains unchanged except near the extreme edges of the plate. A careful measurement of $\ell$, under a microscope, gives the original thickness t, since $t = \ell \tan \theta$.

Plates were exposed to a weak beam of alpha-particles and left undeveloped. Such plates were subsequently used in the experiment. Thus each plate which was scanned for mesons had a sufficient number of easily recognizable "calibration tracks" from which the true thickness of the emulsion was obtained. Emulsion thicknesses are easily measured by this method to $\pm$ 3 percent.

# V CORRECTIONS

A number of the quantities entering into the cross section formula IV-14 require corrections. This is the subject of the present section.

## V-1. Decay in flight

A certain fraction of the positive and negative $\pi$ mesons produced in the target will decay into positive and negative $\mu$ mesons before coming to the end of their ranges. The observed number of mesons must be corrected for this effect.

The half-life for negative $\pi$-$\mu$ decay has been measured by Richardson[1] who obtained a value of $(0.77 \pm {}^{.21}_{.15}) \times 10^{-8}$ sec. Martinelli and Panofsky[2] measured the positive $\pi$-$\mu$ half-life and obtained $(1.37\ {}^{+.10}_{-.12}) \times 10^{-8}$ sec. Nevertheless it is generally assumed that both positive and negative $\pi$ mesons have the same half life for $\pi$-$\mu$ decay. It will be seen later that the correction for decay in flight is of the order of 2-3 percent. It is therefore relatively unimportant which value of the half-life is chosen for purposes of this correction. In the following calculation we use $1.37 \times 10^{-8}$ sec. It should be noted that this value of the half-life applies to the rest-system of the meson.

The time taken by a meson to traverse a distance equal to its range, the time being measured in the meson's frame of reference, is

$$t = \int_0^R \sqrt{1-\beta^2}\ \frac{dx}{\beta c} \qquad \text{V-1}$$

where $\beta = v/c$, v is the velocity of the meson, and R is its total range. $\beta$ is a function of x, since the meson is constantly losing

energy during its passage through the material.

The kinetic energy of the meson as a function of x, the distance into the absorber, is

$$T(x) = T\left[R(T_o) - x\right] \qquad \text{V-2}$$

where $R(T_o)$ is the range corresponding to an initial energy $T_o$. Now

$$T(x) = m_o c^2 \left[\frac{1}{\sqrt{1-\beta^2}} - 1\right] \qquad \text{V-3}$$

where $m_o$ is the rest mass of the $\pi$ meson. Hence

$$\frac{\sqrt{1-\beta^2}}{\beta c} = \frac{m_o c}{\sqrt{T(x)\left[T(x) + 2m_o c^2\right]}} \qquad \text{V-4}$$

and

$$t = \int_0^R \frac{m_o c\,dx}{\sqrt{T(x)\left[T(x) + 2m_o c^2\right]}}$$

T(x) is most easily obtained from a range-energy curve for $\pi$ mesons. The integration is performed numerically.

A meson in going from the target to the emulsion traverses 7.15 cm of air and enters an aluminum absorber, 2.5 cm thick. If the meson's original energy is greater than 37 Mev, it will continue into a copper absorber and eventually stop.

Fig. V-1 gives a plot of $\lambda t$ as a function of meson energy where $\lambda$ is the meson decay constant and t is the total time taken by the meson in going from target to emulsion. It is seen that the correction is largest for low energy mesons, about 3.5 percent at 10 Mev, and smallest, about 2 percent, at 90 Mev. Had we used Richardson's value for the half-life the corrections would be increased by a factor of about 1.8.

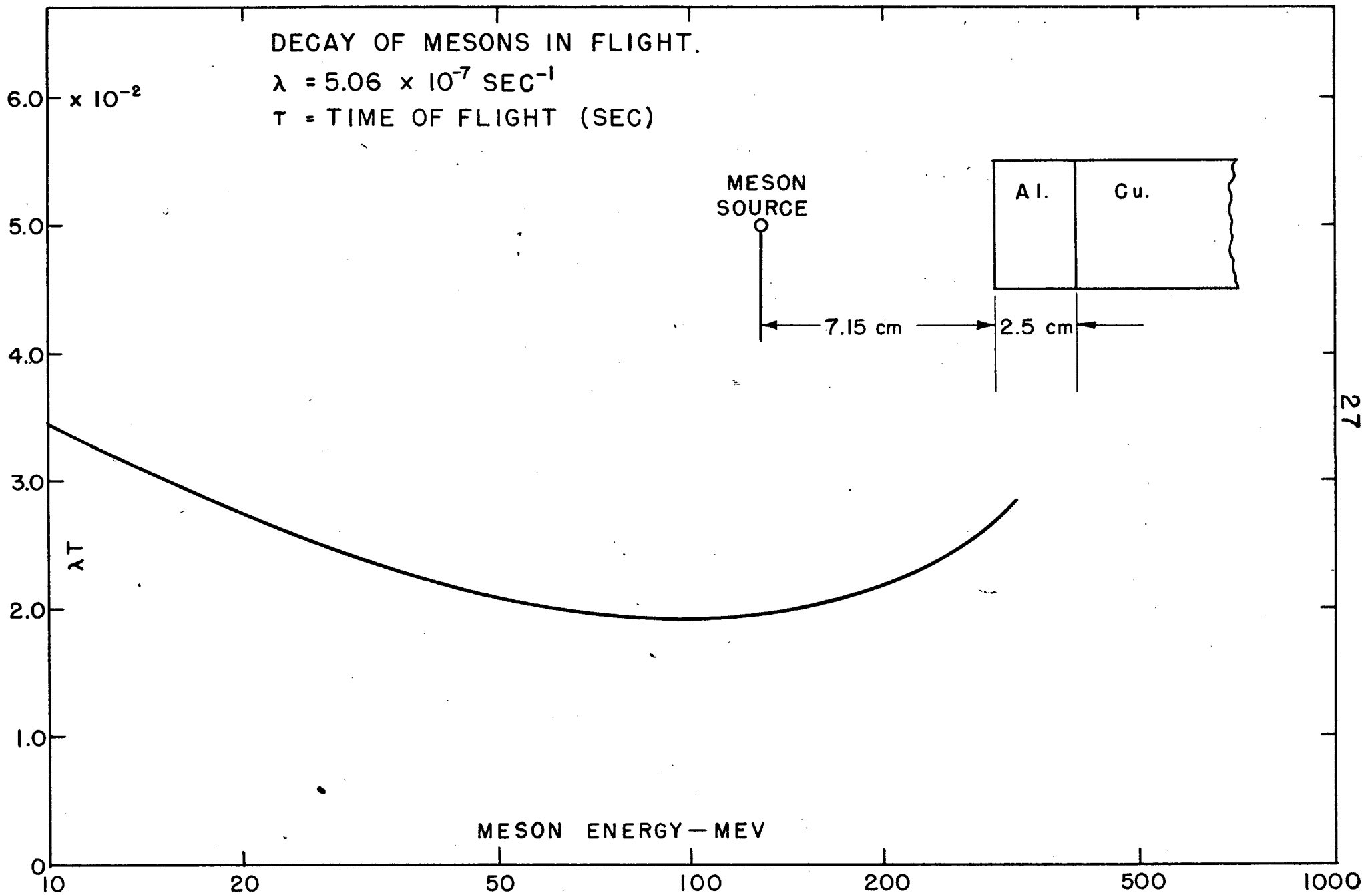


FIG. V-1

14465-1

The curve of $\lambda t$ vs. meson energy (Fig. V-1) has a minimum at about 90 Mev. That a minimum should exist can be seen from the following simple physical considerations. Low energy mesons require a comparatively long time to traverse the air path of 7.15 cm while the time required to come to rest in the absorber is short. On the other hand, high energy mesons spend a long time in the absorber and only a comparatively short time in the air path. At some intermediate energy, the two effects give rise to a minimum.

V-2. Extended source

As seen from Fig. II-1, the target is inclined at 45° to the direction of the beam. Consequently, mesons are produced at points in the target which are at different distances from a given point on the photographic plate. The largest correction to the solid angle occurs for regions of the plate which are nearest the target. These are the regions in which low energy mesons are found. A careful calculation of the solid angle correction for the worst case, namely for regions in which mesons of about 15 Mev are found, shows that the cross section is to be increased by less than two percent. For mesons of higher energy which are found at points farther removed from the target, the correction is smaller.

V-3. Effective thickness of emulsion

Mesons which come to rest near the upper or lower surface of the emulsion are apt to be improperly identified or missed entirely, particularly if the trajectories of the decay particles make steep angles with the emulsion surface. The practice was therefore adopted of rejecting all mesons ending within 3 microns of either emulsion surface.

In calculating the cross section, the reduced emulsion thickness was used.

V-4. Proton energy loss in the target

The two lead targets used in the course of this experiment had thicknesses of 2.16 and 11.15 $gm/cm^2$ in the direction of the proton beam. For protons of 345 Mev the energy loss in traversing the targets is 3.6 and 18.5 Mev respectively.

In order to correct the observed cross section for the proton energy loss, it is necessary to have an excitation function for meson production in lead. This however does not exist. White and Jones[3] obtained a relative yield function for negative $\pi$ mesons of energies 2-10 Mev produced in carbon by high-energy protons. Assuming the yield curve to be approximately the same for lead and carbon, the average cross section for low-energy negative $\pi$ mesons is reduced by about 1.1 percent. The corrections for higher energy mesons cannot be made but it is expected that they are small in comparison with the statistical errors which are of the order of 15 percent.

V-5. Meson energy loss in the target

Mesons which enter the absorbers in the energy interval between E and $E + \Delta E$, have been created at various depths in the target up to the full thickness t. The original energies of the mesons are distributed between E and $E + \Delta E + \delta$ where $\delta$ is the maximum energy loss in the target. To a first approximation $\delta$ is equal to $(dE/dx)_{E'}t$, where $(dE/dx)_{E'}$ is the rate of energy loss in the target at an energy $E' = E + \frac{\Delta E}{2}$. Thus the mid-point of the observed energy interval, namely $E + \frac{\Delta E}{2}$ is shifted to $E + \frac{\Delta E}{2} + t/2 \left(\frac{dE}{dx}\right)_{E'}$. This is taken to be the mean energy of the mesons.

V-6. Nuclear absorption and scattering

Of all the $\pi$ mesons entering the absorbers, a certain fraction will interact with the nuclei of the absorber and will be absorbed or scattered through large angles. Clearly the observed production cross section must be corrected for this effect. However, the cross sections for such interactions have not been measured and the corrections cannot be made with any accuracy. It has been estimated[4] that the cross section for nuclear absorption and scattering is of the order of the geometrical cross section of the nucleus. Assuming this to be the case, we have $\sigma(A\ell) = 5.9 \times 10^{-25}$ cm$^2$ and $\sigma(Cu) = 10.5 \times 10^{-25}$ cm$^2$. For mesons up to 60 Mev, the correction remains smaller than the probable error due to statistics alone. Beyond that energy the percent corrections become larger, about 50 percent at 100 Mev, but as will be shown in Section VI, the cross-section for the production of mesons of energies higher than 60 Mev drops rapidly. Consequently, the general shape of the positive and negative spectra and the integrated values of the cross sections are not materially influenced. Nevertheless, when the absorption and scattering cross sections become known, the present data can be corrected.

V-7. Mesons produced in absorbers

Bombardment of a target with high energy protons results in the emission of various radiations in addition to mesons. This radiation largely consists of protons and neutrons. Among these particles there will be some of sufficient energy such that if they enter the absorber they may produce mesons which can appear on the photographic plate. Clearly in estimating this effect we are interested only in particles whose energy is above the threshold for meson production, which may be taken to be about 200 Mev. The discussion will be confined to particles

scattered from the target at approximately 90° to the beam direction. It should be noted that diffraction scattering is negligible at 90° since the wave-length of the proton is small in comparison to the radius of the lead nucleus.

If it is assumed that the cross section for the inelastic scattering of neutrons and protons of energies higher than 200 Mev is 0.1 barns, the total number of mesons produced in the target is about 1000 times greater than the number of mesons produced in the absorber by scattered protons and neutrons. The average solid angle for mesons produced in the absorber is about a factor of 10 larger than for mesons produced in the target. On this basis one would say that about 1 percent of the observed mesons have been produced in the absorber.

This is qualitatively verified experimentally insofar as no mesons have been observed which do not come from the general direction of the target.

In this connection it should be mentioned that a background run of several hours duration with the target removed yielded no mesons. In all other respects, the experimental arrangement for the background run was identical to that in which the target was used.

V-8. Small angle scattering

Mesons which enter the emulsion with a residual range such that they would normally stop within the emulsion may, because of small angle scattering, leave before coming to rest. A correction to the observed number of mesons would therefore be required. On the other hand mesons which would normally stop in the absorber or glass backing of the photographic plate may, for the same reason, be scattered into the emulsion. Thus the correction is largely compensated since the scattering properties of a

material depend on $\sqrt{Z}$ and this is not far different for all three materials.

## VI CALCULATIONS AND RESULTS

The cross section formula was given by Equation IV - 14.

$$\frac{d\sigma}{dEd\Omega}(E,\theta) = \frac{AeN_0r^2}{L\rho t_t Q t \frac{Ra}{Re} \sec\alpha\Delta E}$$

A is the atomic weight of lead = 207.21, e is the proton charge = $1.602 \times 10^{-19}$ coulombs; L is the Avogadro number = $6.023 \times 10^{23}$ mole$^{-1}$, $\alpha$ is the angle of inclination of the photographic plate (Fig. IV - 1) = 15°, $\rho t_t$ is the surface density of the target = 2.158 gm/cm$^2$ for the thin target and 11.15 gm/cm$^2$ for the thick target. These were obtained by accurately weighing the targets and measuring their dimensions.

Ra/Re is the ratio of the range of the $\pi$ meson in the absorber to its range in emulsion. The absorbers used were made of aluminum and copper. Range energy curves[1] for $\pi$ mesons in these materials were obtained by transforming existing range-energy curves for protons. The transformation is

$$R_\pi(E) = \frac{m_\pi}{m_p} R_p\left(\frac{m_p}{m_\pi} E\right)$$

where $R_\pi(E)$ is the range of a $\pi$ meson of energy E, $m_\pi$ and $m_p$ are the masses of the $\pi$ meson and the proton respectively, and $R_p$ is the range of the proton, $m_p/m_\pi = 6.45$.[2] A range-energy curve for protons in emulsion is given by Barkas[3] et al. which is transformed as above. The range-energy curves are considered to be accurate to 2 percent. The quantity $(R_a/R_e)$ sec. 15° is 1.098 for an emulsion embedded in aluminum and 0.405 for emulsion in copper. These numbers were evaluated for mesons of a few Mev.

Q is the charge accumulated by the integrator in the course of a run, as discussed in Section II.

t is the undeveloped emulsion thickness measured by the method described in Section IV. By means of a scale on the fine focus control of the microscope it was possible to measure the developed emulsion thickness and determine a shrinkage factor. Six microns were subtracted from the developed thickness, as discussed in Section IV - 3, and the result reconverted to emulsion thickness prior to development. These measurements were made on each plate separately with an estimated accuracy of 3 percent.

$\ell$ is the transverse length of the volume scanned (Fig. IV-1). It was measured by means of a carefully built microscope stage* equipped with a micrometer-type drive which could be read to 2 microns.

$\Delta E$ is the energy interval chosen for scanning. It is directly given by the coordinates of the region scanned since these determine the thickness of absorbing material traversed by the mesons in order to stop in the area of the plate being observed. An accurate determination of $\Delta E$ from the coordinates is obtained with the help of a dE/dx curve for $\pi$ mesons in the material of the absorber. The latter is obtained from a corresponding curve for protons via the transformation

$$\left[\frac{dE}{dx}(E)\right]_{\pi} = \left[\frac{dE}{dx}\left(\frac{m_p}{m_{\pi}} E\right)\right]_p$$

$\Delta E$ varied from 5-10 Mev in different regions of the spectrum. The energy E is taken at the mid-point of the interval $\Delta E$ and the correction for loss of energy in the target, as discussed in Section V-5 is easily

---

* The microscope stage was designed and built by Mr. W. M. Brower.

made with a dE/dx curve, for $\pi$ mesons in lead. The thin target, of surface density 2.158 gm/cm$^2$ was used for low energy mesons up to 46 Mev. This resulted in an increase in E of from 2 to 4 Mev. Higher energy mesons were obtained from the thick target of surface density 11.15 gm/cm$^2$ with a resultant increase in E of 5 to 8 Mev.

r is the distance from the center of the target to the mid-point of the energy interval scanned on the photographic plate, the distance being measured along a line at 90° to the direction of the beam. The region scanned was always centrally located with respect to this line so that the angle of observation, $\theta$, was 90° with a symmetrical angular spread of $\pm$ 2.5° to $\pm$ 12° for different energy mesons. The average value of $1/r^2$, taking into account the finite extent of the target and the region scanned, deviated by no more than 2 percent from the value measured as described above. The distance from the center of the target to the nearest absorber was 7.15 cm. The value of r is therefore 7.15 cm plus the range of the meson in the absorbing material.

$N_o$ is the number of mesons found in the volume scanned. All scanning was done with a good quality binocular microscope equipped with an oil immersion lens giving a total magnification of about 500. The diameter of a field of view, under oil, was about 220 microns. The negative mesons are multiplied by factor 1.37 (Section III); the new total is corrected for decay in flight in the manner discussed in Section V-1. Corrections for the variation of cross section with proton energy, nuclear absorption and scattering, for mesons produced in absorbers, and for small angle scattering are not made.

The data for the combined spectrum of positive and negative mesons are given in Table VI-1 and plotted in Fig. VI-1. The spectrum has a

Table VI-1 Combined Spectrum of Positive and Negative $\pi$ Mesons

| E Mev | $N_0(\pi^+, \pi^-)$ | $\frac{d\sigma}{dEd\Omega}$ ($\times 10^{-30}$) cm$^2$/Mev x ster. x nucleus |
|---|---|---|
| 17.9 | 11.2 | 10.4 ± 2.1 |
| 30.0 | 20.4 | 21.0 ± 3.1 |
| 46.1 | 23.7 | 18.7 ± 2.6 |
| 63 | 22.3 | 9.2 ± 1.3 |
| 82 | 20.8 | 4.4 ± .6 |
| 101 | 7.1 | 0.88 ± .25 |
| 120 | 2.0 | 0.31 ± .15 |

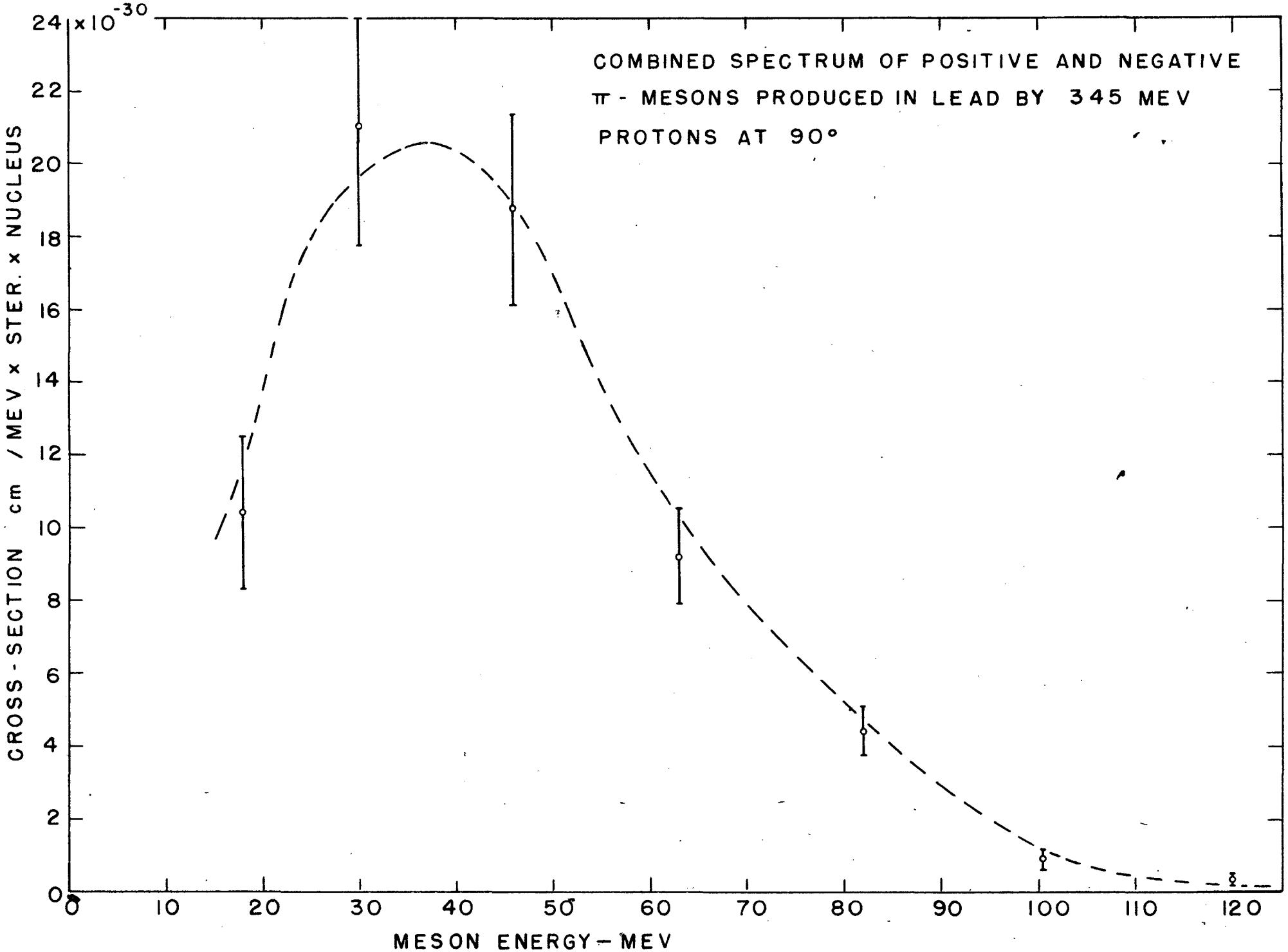


FIG VI - 1

14471-1

peak at about 37 Mev with a corresponding cross section of $(20.5 \pm 3) \times 10^{-30}$ cm$^2$ (steradian)$^{-1}$ (Mev)$^{-1}$ (nucleus)$^{-1}$. Mesons with energies up to 120 Mev were observed. In all cases probable errors are indicated. Of greater fundamental interest than the combined spectrum are the separate positive and negative spectra. The data are shown in Table VI-2 and in Figs. VI-2, 3. The positive spectrum extends to 120 Mev with a maximum at about 40 Mev where the cross section is $(11.8 \pm 2) \times 10^{-30}$ cm$^2$ (steradian)$^{-1}$ (Mev)$^{-1}$ (nucleus)$^{-1}$. The highest energy negative mesons found were at 82 Mev, although they were looked for at 101 and 120 Mev where a number of positive mesons were found. At these two energies, the points are indicated with a probable error based on the probability of having found some mesons within the volume scanned. The maximum of the negative spectrum occurs at about 30 Mev with a cross section of $(11.5 \pm 2) \times 10^{-30}$ cm$^2$ (steradian)$^{-1}$ (Mev)$^{-1}$ (nucleus)$^{-1}$. A comparison of the shapes of the positive, negative and combined spectra is shown in Fig. VI-4. It is to be observed that for positive mesons, the maximum cross section occurs at an energy which is about 10 Mev higher than the maximum for negative mesons. This shift in the peaks of the two spectra is probably influenced by the Coulomb barrier of the lead nucleus which is about 15 Mev for singly charged particles. The maximum value of the cross section for positive mesons is approximately equal to the maximum value for negative mesons.

The combined spectrum, when integrated over the total range of meson energies, gives a differential cross section, $d\sigma/d\Omega$, of $(10.3 \pm 1.6) \times 10^{-28}$ cm$^2$ (steradian)$^{-1}$ (nucleus)$^{-1}$. Considering positive and negative mesons separately the differential cross section is $(6.0 \pm 1.1)$

Table VI-2 Positive and Negative Spectra of $\pi$ Mesons

| $\frac{E}{Mev}$ | $N_o(\pi^+)$ | $\frac{d\sigma^+}{dEd\Omega}$ (x $10^{-30}$) / $cm^2$/Mev x ster. x nucleus | $N_o(\pi^-)$ | $\frac{d\sigma^-}{dEd\Omega}$ (x$10^{-30}$) / $cm^2$/Mev x ster. x nucleus |
|---|---|---|---|---|
| 17.9 | 4.1 | 3.8 ± 1.3 | 7.1 | 6.6 ± 1.7 |
| 30.0 | 9.2 | 9.5 ± 2.1 | 11.2 | 11.5 ± 2.3 |
| 46.1 | 15.3 | 12.1 ± 2.1 | 8.4 | 6.6 ± 1.5 |
| 63 | 15.4 | 6.3 ± 1.1 | 6.9 | 2.9 ± 0.7 |
| 82 | 19.4 | 4.1 ± 0.6 | 1.4 | 0.3 ± 0.2 |
| 101 | 7.1 | 0.88 ± 0.25 | 0 | $0.0 \pm {}_{0}^{.08}$ |
| 120 | 2.0 | 0.31 ± 0.15 | 0 | $0.0 \pm {}_{0}^{.10}$ |

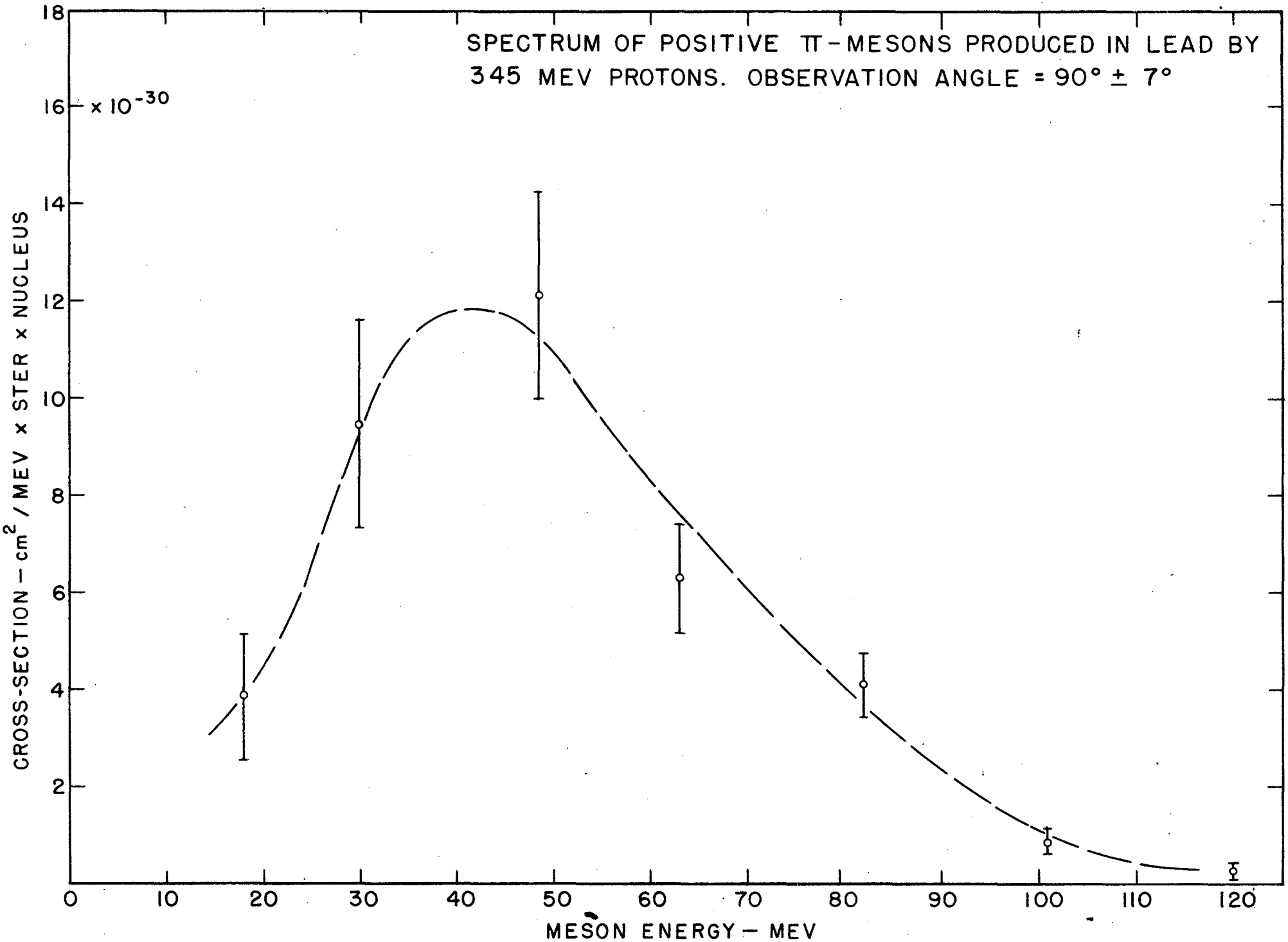


FIG. VI-2

14426-1

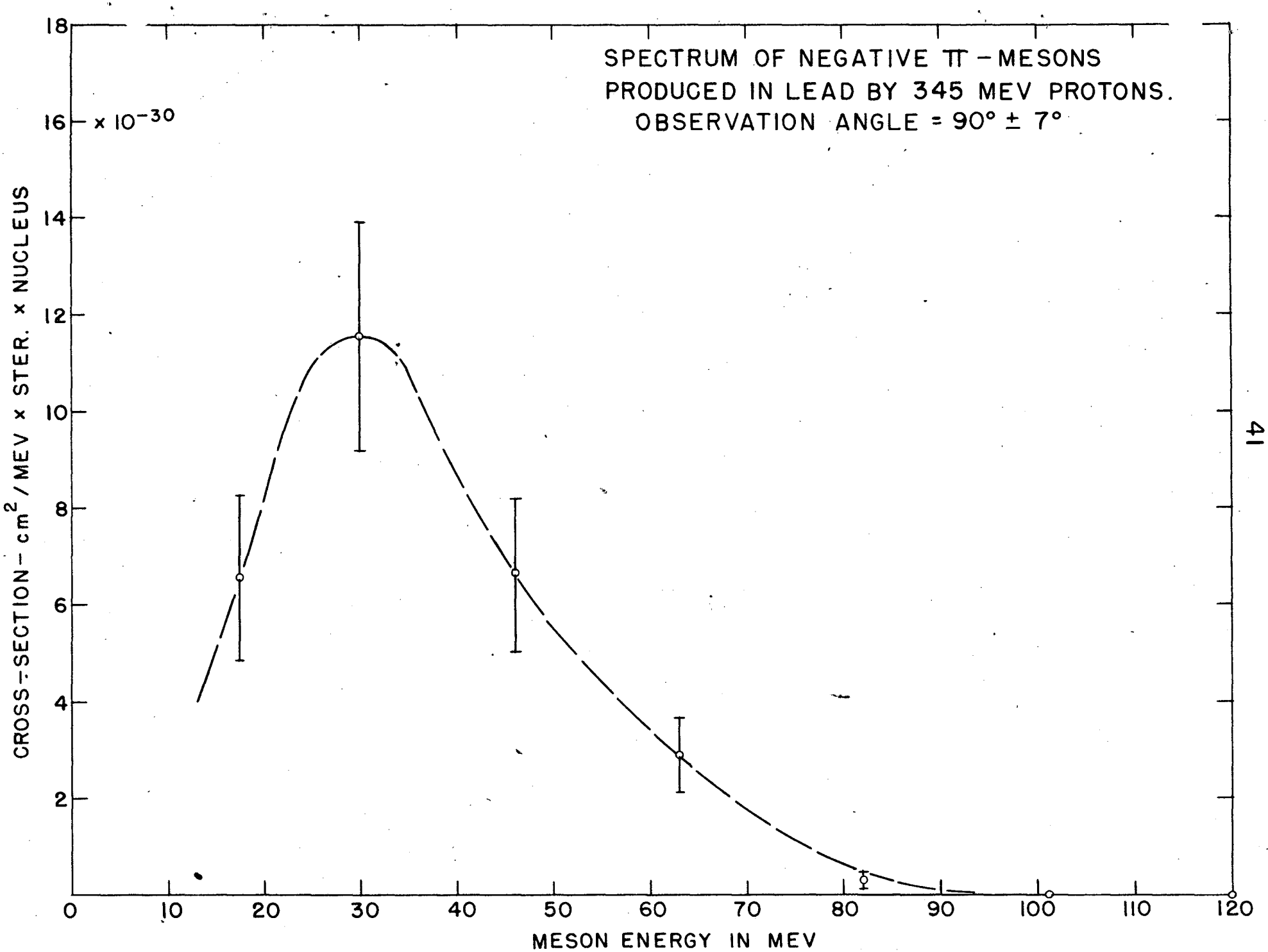


FIG. VI - 3

14425-1

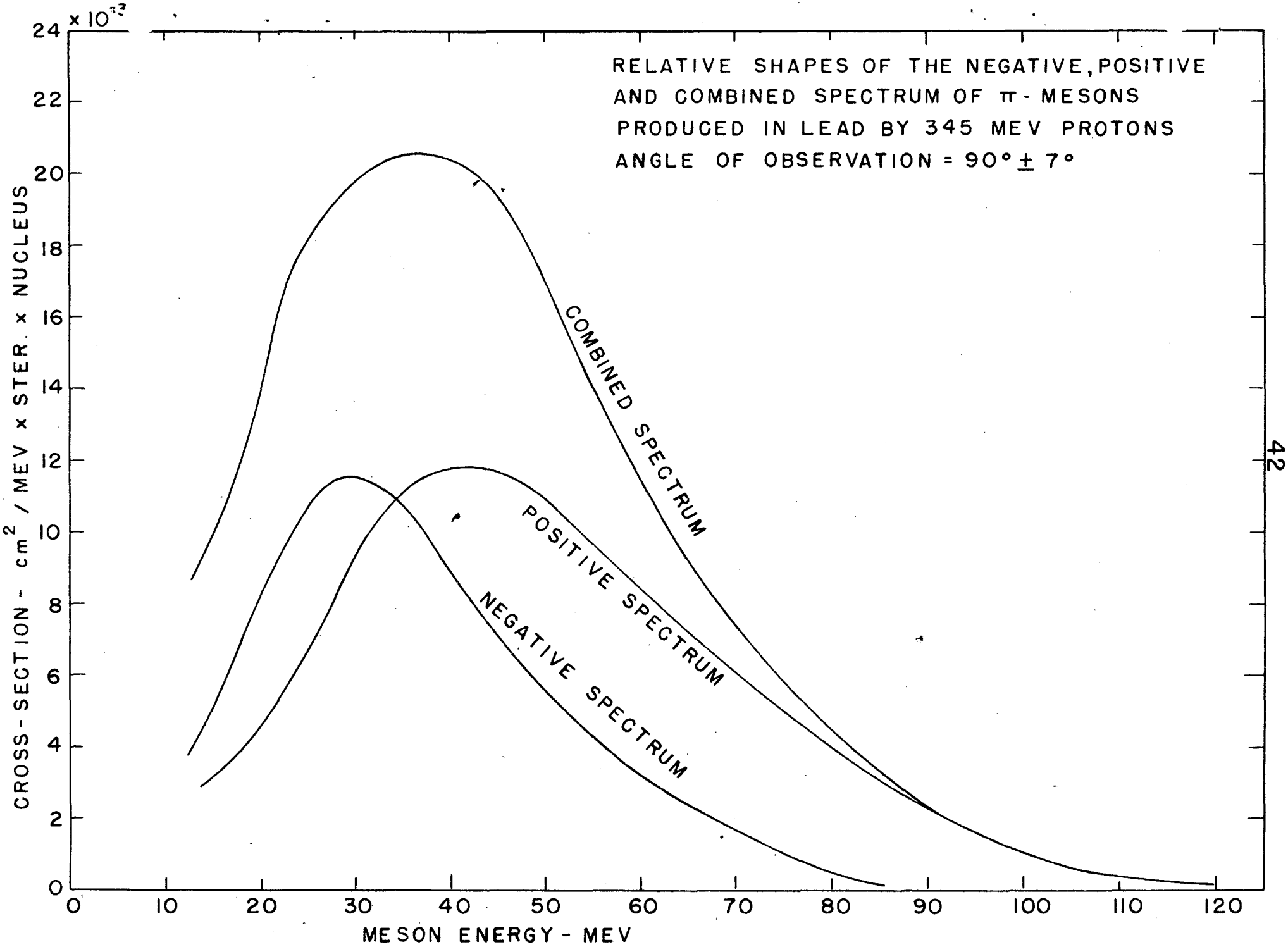


FIG. VI - 4



14467-1

x $10^{-28}$ $cm^2$ $(steradian)^{-1}$ $(nucleus)^{-1}$ for positives and $(4.3 \pm 1.9)$ x$10^{-28}$ $cm^2$ $(steradian)^{-1}$ $(nucleus)^{-1}$ for negatives. The total cross section for the production of mesons would be obtained by integrating over the angular distribution. The latter is however not known at present. If one assumes spherical symmetry an estimate of the total cross section for the production of positive and negative mesons is 0.01 barns. The ratio of the differential cross section for positive mesons to that for negative mesons is $1.4 \pm .6$.

It is of interest to investigate the variation of the relative production of positive and negative mesons as a function of meson energy. The ratio of negative to positive mesons is tabulated in Table VI-3 and plotted in Fig. VI-5. The statistics are too poor to define the details of the energy dependence but it is clear that for low energy mesons of about 18 Mev, the number of negative mesons produced is about equal to the number of positive mesons. At higher energies, mostly positive mesons are produced.

The comparison of the characteristics of meson production in lead with those for carbon, the latter obtained by Richman and Wilcox[4] is summarized in Table VI-4. For purposes of visual comparison, the carbon and lead spectra are plotted together in Figs. VI-6,7. The cross sections have been divided by their respective values of $A^{2/3}$ namely 5.25 for carbon and 35.0 for lead. Comparing the positive spectra, it is seen that mesons from carbon extend to somewhat higher energies, but the general shapes are quite similar. Comparing the cross sections integrated over meson energies it is seen that $\frac{d\sigma^+/d\Omega\,(Pb)}{d\sigma^+/d\Omega\,(C)} = 3.0 \pm .6$ whereas $\frac{A^{2/3}\,(Pb)}{A^{2/3}\,(C)} = 6.76$. Thus the increase of cross section with the mass number of the

Table VI-3 Ratio of Negative to Positive $\pi$ Mesons

| $\frac{E}{Mev}$ | $N(\pi^-)/N(\pi^+)$ |
|---|---|
| 17.9 | $1.7 \pm .7$ |
| 30.0 | $1.2 \pm .4$ |
| 46.1 | $0.55 \pm .16$ |
| 63 | $0.46 \pm .14$ |
| 82 | $0.07 \pm .04$ |
| 101 | $0 \pm {}^{.1}_{0}$ |
| 120 | $0 \pm {}^{.3}_{0}$ |

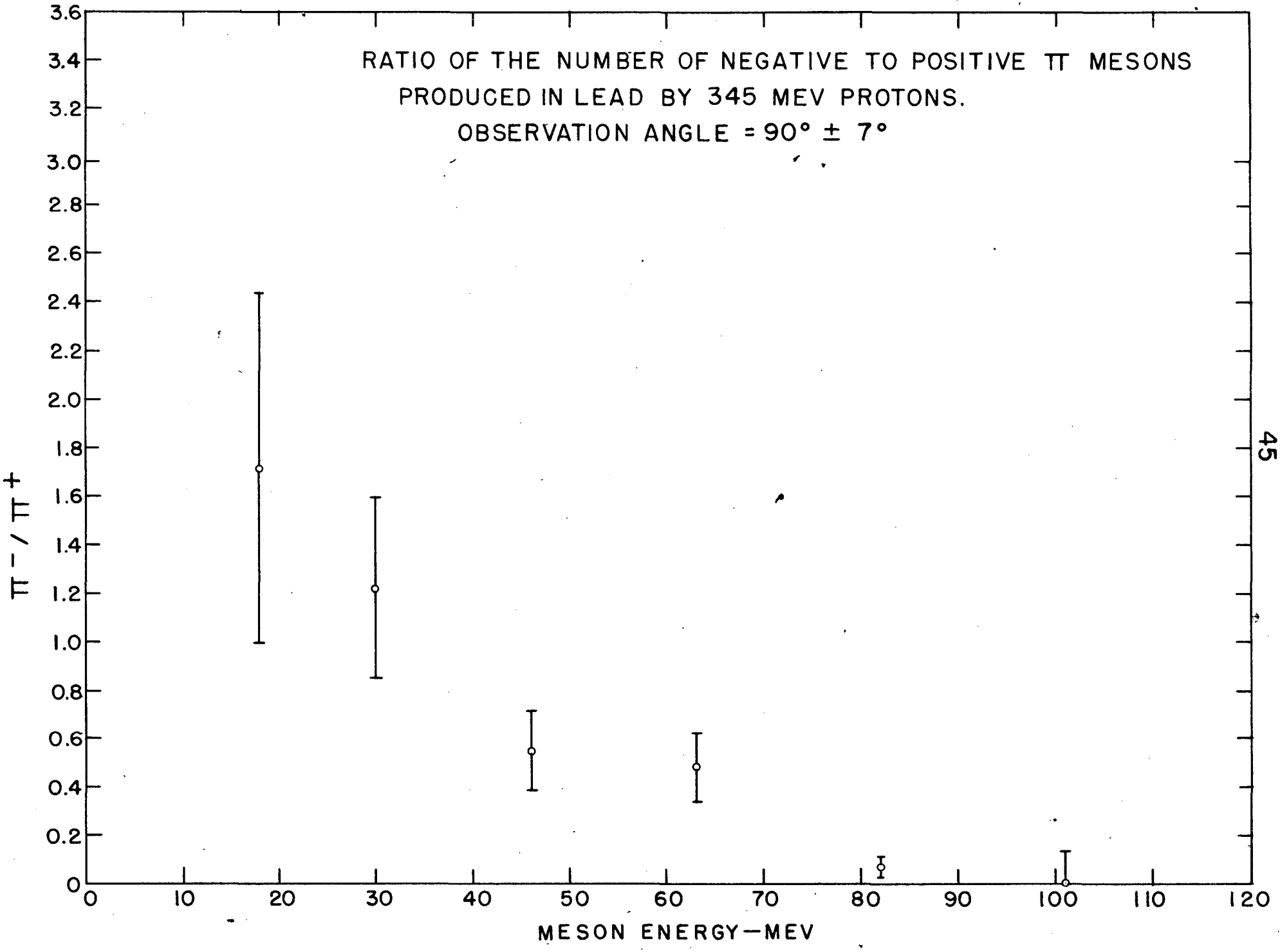


FIG. VI-5

14424-1

Table VI-4 Characteristics of the Production of $\pi$ Mesons in Lead and Carbon

| | Pb | C | C | Pb/C |
|---|---|---|---|---|
| Upper end of positive spectrum (Mev) | ~120 | | ~135 | |
| Upper end of negative spectrum (Mev) | ~ 90 | | ~115 | |
| Energy of maximum cross section for positive mesons (Mev) | ~40 | | ~40 | |
| Maximum cross section for positive mesons ($cm^2$ ster.$^{-1}$ Mev$^{-1}$ | $(11.8 \pm 2) \times 10^{-30}$ | | $(2.8 \pm .3) \times 10^{-30}$ | $4.2 \pm .8$ |
| Energy of maximum cross section for negative mesons (Mev) | ~30 | | ~35 | |
| Maximum cross section for negative mesons ($cm^2$ ster.$^{-1}$ Mev$^{-1}$ nucleus$^{-1}$) | $(11.5 \& 2) \times 10^{-30}$ | | $(0.62 \pm .1) \times 10^{-30}$ | $18.5 \pm 5.1$ |
| Positive mesons cross section integrated over meson energy, $\frac{d\sigma^+}{d\Omega}$, ($cm^2$ ster.$^{-1}$ nucleus$^{-1}$) | $(6.0 \pm 1.1) \times 10^{-28}$ | | $(2.0 \pm .2) \times 10^{-28}$ | $3.0 \pm .6$ |
| Negative meson cross section integrated over meson energy, $\frac{d\sigma^-}{d\Omega}$, ($cm^2$ ster.$^{-1}$ nucleus$^{-1}$) | $(4.3 \pm 1.9) \times 10^{-28}$ | | $(0.4 \pm 0.1) \times 10^{-28}$ | $10.7 \pm 5$ |
| $\frac{d\sigma^+/d\Omega}{d\sigma^-/d\Omega}$ | $1.4 \pm .6$ | | $5 \pm 1.4$ | |
| $A^{2/3}$ | 35.0 | | 5.25 | 6.7 |

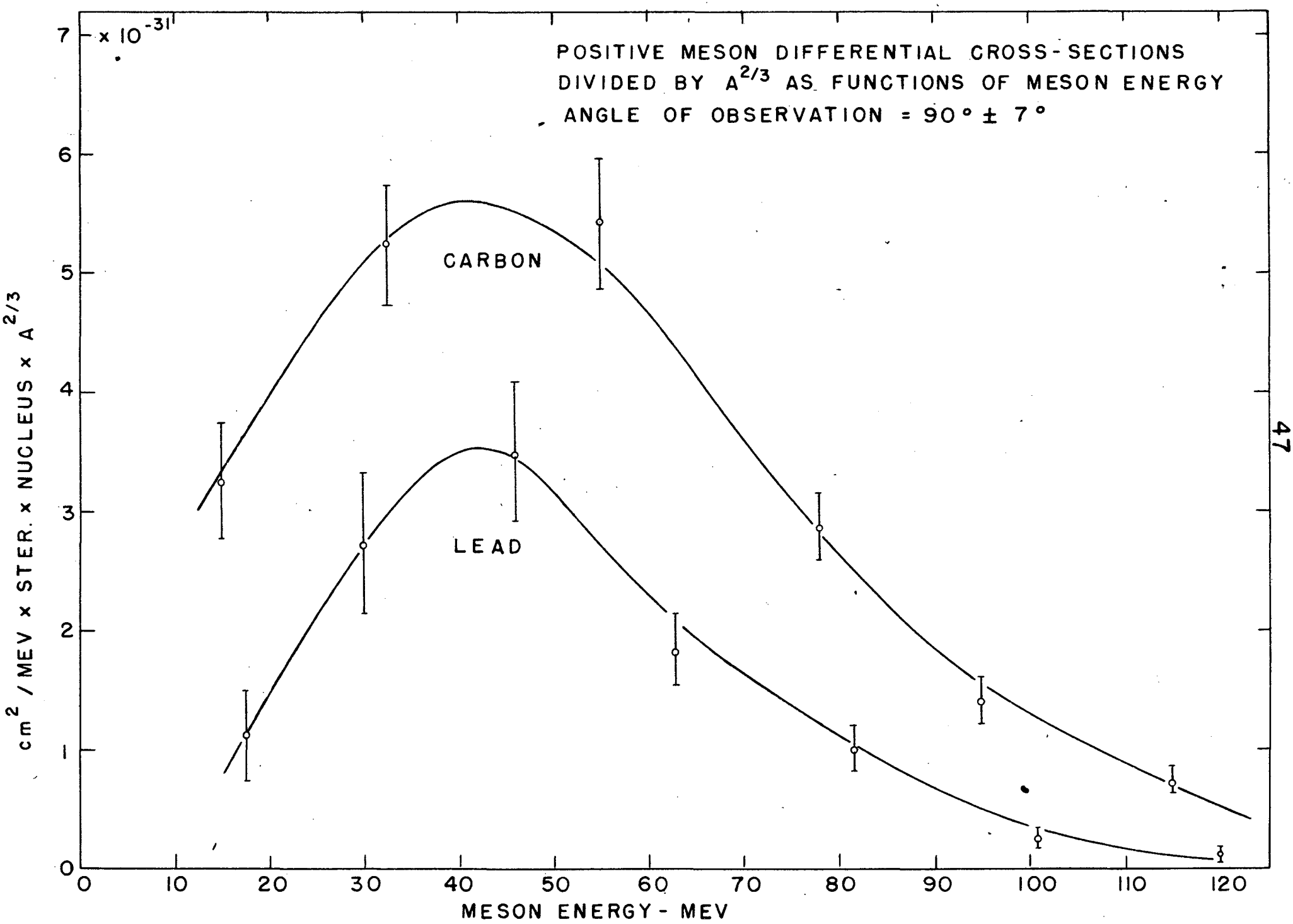


FIG. VI - 6

1446 851

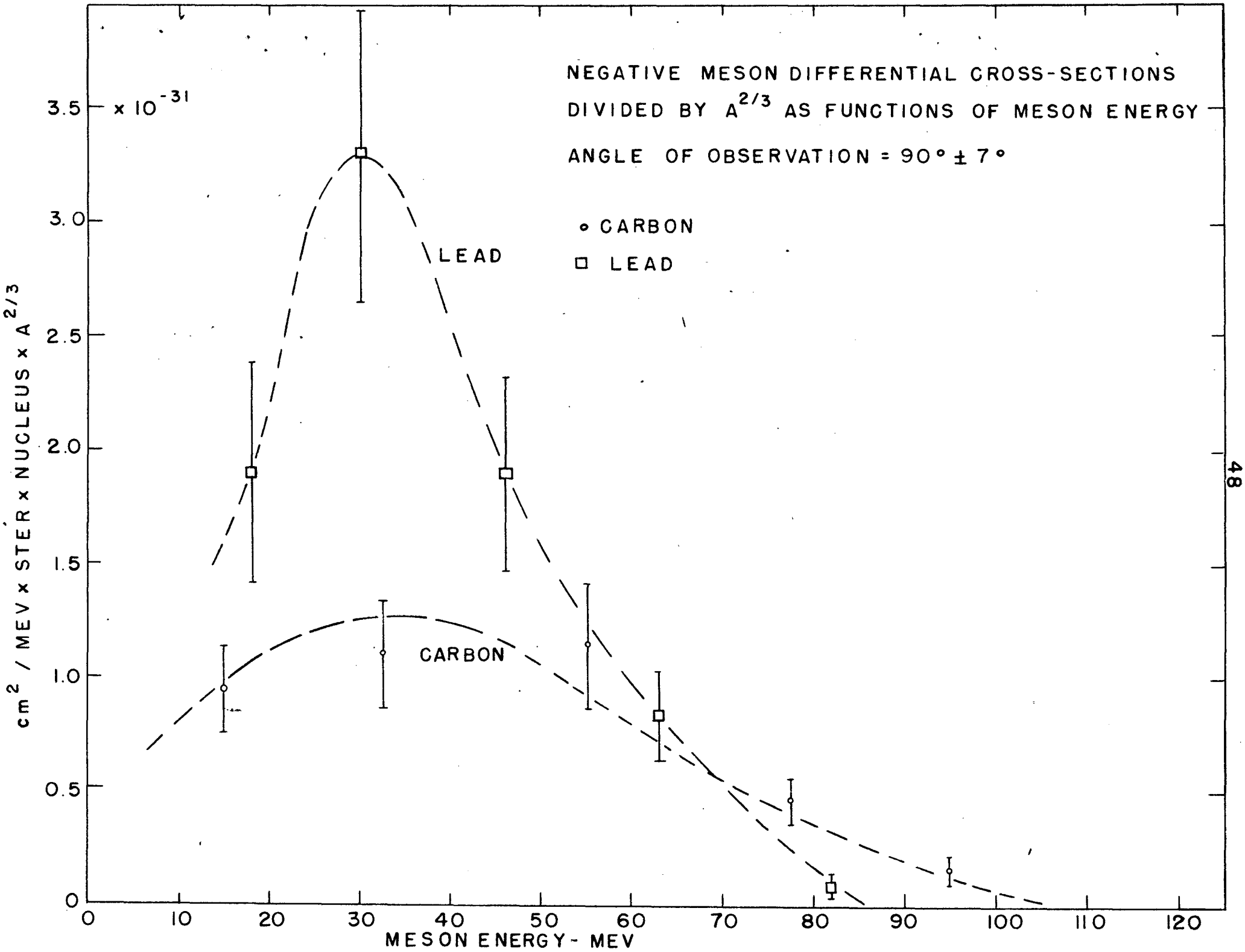
NEGATIVE MESON DIFFERENTIAL CROSS-SECTIONS
DIVIDED BY $A^{2/3}$ AS FUNCTIONS OF MESON ENERGY
ANGLE OF OBSERVATION = 90° ± 7°
∘ CARBON
□ LEAD
LEAD
CARBON
$\times 10^{-31}$
$cm^2$ / MEV × STER × NUCLEUS × $A^{2/3}$
3.5
3.0
2.5
2.0
1.5
1.0
0.5
0
0
10
20
30
40
50
60
70
80
90
100
110
120
MESON ENERGY - MEV

FIG. VI - 7

nucleus is considerably slower than as $A^{2/3}$. For the negative mesons, a different situation exists, the integrated cross section increases more rapidly than as $A^{2/3}$; in fact within the probable errors the cross section increases proportionately to the mass number. This fact is reflected in the ratio $\frac{d\sigma^+/d\Omega}{d\sigma^-/d\Omega}$ which is $1.4 \pm .6$ for lead and $5 \pm 1.4$ for carbon.

Theoretical calculations on the characteristics of meson production in light and heavy nuclei have been made by Taylor and Chew[5] and by Chew and Steinberger.[6]

The momentum distribution of the nucleons in a heavy nucleus was calculated to be a degenerate Fermi gas of neutrons and protons. The matrix element governing the process of meson production was assumed to be constant. A value of the coupling constant, g, was chosen such that $g^2/\hbar c = 0.3$, although the results are insensitive to variations in $g^2/\hbar c$ from about 0.25 to 0.75. Calculations of meson production from free nucleons at rest show that the mesons are produced primarily in the forward direction with comparatively few mesons, and of low energy, produced at $90^\circ$ to the direction of the beam. Hence the calculated meson spectrum from a complex nucleus, at $90^\circ$, depends rather strongly on the assumed momentum distribution of the nucleons in the nucleus.

The results of these calculations predict the energy and angular distributions of the $\pi$ mesons from a heavy nucleus such as lead. The angular distributions were not determined in this experiment. Considering the energy distribution at $90^\circ$, the theoretical values of the absolute cross section are uncertain because they depend on the cube of $g^2/\hbar c$

which, in itself, is uncertain. Furthermore, the theoretical calculations do not take into account Coulomb effects, nor do they distinguish between the production of positive and negative mesons in any other way. Since the observed spectra (Fig. VI-4) of positive and negative mesons differ in several respects, it is not entirely clear how the comparison between theory and experiment should be made. On the other hand, the shape of the calculated spectrum fits the observed positive spectrum for meson energies higher than about 40 Mev. Since Coulomb effects have been ignored in the calculations, agreement cannot be expected in the low energy portion of the spectrum. With regard to negative mesons, the upper end of the spectrum is influenced by the Pauli exclusion principle in the following way: First it is reasonable to assume that a given proton in the nucleus is generally surrounded by two neutrons and another proton of opposite spin. The production of negative mesons by protons may be considered via the elementary reaction

$$1. \quad p + n \longrightarrow p + p + \pi^-$$

It is seen that the original configuration of 2 protons and 2 neutrons now consists of 4 protons and 1 neutron. If the negative meson is of high energy all the protons must be left in low energy states, some of which, however, are already occupied. This results in an inhibition on the formation of high energy negative mesons. Positive mesons, on the other hand, may be produced in two ways

$$2. \quad p + p \longrightarrow p + n + \pi^+$$

$$3. \quad p + n \longrightarrow n + n + \pi^+.$$

Whichever interaction occurs, the original configuration of 2 protons

and 2 neutrons becomes 2 protons and 3 neutrons. When a high energy positive meson is formed, there is again competition among the 3 neutrons for low momentum states, but this is not as severe as is the competition among the 4 protons when a high energy negative meson is produced.

On the basis of the above three reactions, alone, one would predict that the ratio of positive to negative mesons is greater than unity. In fact, if exclusion principle arguments, Coulomb effects, etc. are ignored, and the nucleus contained an equal number of protons and neutrons one might assign relative a priori probabilities to (1), (2) and (3) of 0.25, 0.50 and 0.25 respectively. Thus the positive to negative ratio would be 3. However, coulomb effects suppress the production of low energy positive mesons and the Pauli exclusion principle, discussed above, suppresses the production of high energy negative mesons. Thus the positive to negative ratio is expected to be a function of meson energy. This qualitative result is in fact borne out by the experiment (Fig. VI-5) as discussed previously.

In comparing the results from lead with those from carbon several points of difference have been noted which may be qualitatively understood in the light of previous remarks. On the basis of the uncertainty principle, a small nucleus such as carbon is expected to have nucleons with higher components of momentum than is the case in lead because the nucleons in carbon are more localized than in lead. Consequently, the meson spectrum from carbon would be expected to extend to higher energies than in the case of lead, even though the recoil energy is greater for the carbon nucleus than for the lead. The fact that relatively more negative mesons are produced in lead than in carbon is attributed to two effects. First,

lead contains about one and a half times as many neutrons as protons in comparison to a neutron-proton ratio of 1 in carbon, and, as mentioned above, negative mesons can be formed only in p-n encounters. Second, since the Coulomb barrier suppresses low energy positive mesons, the effect is more pronounced in lead with a barrier height of about 15 Mev than in carbon with a barrier height of about 5 Mev. The prediction of the manner in which the cross sections should depend on mass number is complicated by various factors such as nuclear transparency, possible scattering or re-absorption of mesons in the parent nucleus which have not been taken into account.

## VII The Wentzel Experiment

Wentzel[1] has suggested an experiment, designed to give information regarding the spin of the $\pi$ meson. It appeared that the experimental arrangement described in Section II was suitable for obtaining the type of information suggested by Wentzel. It was therefore felt that insofar as it was perhaps possible to test Wentzel's suggestions without sacrificing the primary object of the experiment, namely the production cross sections of mesons in lead, this should be done. Wentzel's experiment may be described as follows.

If it is assumed that $\pi$ mesons have unit spin; such mesons produced in nucleon-nucleon collision may be polarized. The type and degree of polarization depends on the matrix element which characterizes meson production. In the disintegration of the polarized $\pi$ mesons into $\mu$ mesons and neutrinos, it is expected that the angular distribution of the $\mu$ mesons will be assymmetric. Wentzel shows that the probability that a $\mu$ meson is emitted into the solid angle d , in the rest system of the $\pi$ meson is

$$P d\Omega = \text{constant } d\Omega \left(1 \pm \frac{v_\mu}{c} \cos 2\theta\right)$$

where $v_\mu$ is the velocity of the $\mu$ meson. From conservation of momentum and energy, and assuming that the rest mass of the neutrino is zero

$$v_\mu = c \frac{m_\pi{}^2 - m_\mu{}^2}{2 m_\pi m_\mu}$$

where $m_\pi$ and $m_\mu$ are the rest masses of the $\pi$ and $\mu$ mesons respectively. The positive sign refers to transverse coupling and the negative sign to longitudinal coupling. $\theta$ is the angle which the direction of emission of the $\mu$ meson forms with the polarization vector of the $\pi$ meson.

From the known masses of the $\pi$ and $\mu$ mesons, $v_\mu/C = 0.27$ and the optimum anisotropy, $(1 + v_\mu/C)/(1 - v_\mu/C)$, is 1.74.

According to Wentzel, it is required that the bombarding energy be close to the threshold for meson production so that the velocities of the meson and nucleon in the final state remain small in comparison with the initial nucleon velocity. Furthermore, in order to avoid depolarization, the magnetic field in the region of observation should be less than 100 gauss. Depolarization from the slowing down of mesons in matter is calculated to be small for low energy mesons.

The experiment therefore consisted of a measurement of the angular distribution of the $\mu$ mesons in $\pi$-$\mu$ decay with the proton beam velocity as the reference direction. As is seen from Fig. II-1, the photographic plates were oriented with their planes parallel to the beam direction. Thus, longitudinally polarized $\pi$ mesons will enter the plate with their spin vectors in the plane of the emulsion. This is the most favorable arrangement since the polarization vector is an axis of symmetry for the angular distribution. If the mesons are polarized transversely, the above arrangement is still the most favorable. The magnetic field in the region in which the experiment was conducted was less than 40 gauss.

A tabulation of the number of $\mu$ mesons found in each 45° interval is shown in Table VII-1. An anisotropy of the type discussed by Wentzel would be displayed by the ratio of the number in b, c, f, g to those in a, b, d, e. This ratio is $1.04 \pm .14$. Furthermore, the number of mesons emitted in the forward direction to the proton beam should be equal to the number emitted in the backward direction, regardless of any considerations of polarization. That this is the case is seen by taking the ratio of

Table VII-1

Angular Distribution of

$\mu$ Mesons in $\pi$-$\mu$ Decay

| | | | |
|---|---|---|---|
| a) | 0-45° | : | 12 |
| b) | 45-90° | : | 14 |
| c) | 90-135° | : | 13 |
| d) | 135-180° | : | 15 |
| e) | 180-225° | : | 10 |
| f) | 225-270° | : | 11 |
| g) | 270-315° | : | 14 |
| h) | 315-360° | : | 13 |

mesons in groups g, h, a, b to those in groups c, d, e, f. The ratio is 1.08 $\pm$ .15.

Thus, insofar as this experiment is concerned the angular distribution of the $\mu$ mesons is very nearly isotropic. It is however important to emphasize those features of the experiment which depart from the conditions as laid down by Wentzel. First, the bombarding energy was 345 Mev which is about 150 Mev above the threshold for meson production. Thus the nucleon velocity in the final state is not necessarily small in comparison with the velocity of the bombarding proton. Second, the data discussed above combine the results obtained from mesons over the entire energy spectrum from 0 to 120 Mev. The depolarization of mesons of high energy in coming to rest in a stopping medium may not be negligible.

Possible interpretations of this result are these. Assuming for the moment that $\pi$ meson has unit spin, the anisotropic distribution is obscured if

a. the depolarization effects in bringing the $\pi$ mesons to rest in matter are not negligible,

b. the number of transversely polarized $\pi$ mesons produced in the target is approximately equal to the number which are longitudinally polarized

c. the degree of polarization of the $\pi$ mesons decreases rapidly as the bombarding energy is increased above threshold.

Another interpretation of the results is that the spin of the $\pi$ meson is zero. Such a conclusion could only be drawn by definitely eliminating the previous interpretation. This cannot be done at present.

## VIII ACKNOWLEDGMENTS

It is a great pleasure to acknowledge the help and guidance of Professors H. A. Wilcox and C. Richman who suggested the problem and gave constant encouragement in the course of its execution. Many helpful and stimulating discussions were held with Professor G. F. Chew. The author is indebted to Professor E. O. Lawrence for his interest in this work and to Mr. J. Vale and the cyclotron crew who made the bombardments. This work was performed under the auspices of the Atomic Energy Commission.

## IX References

I-1. E. Gardner and C. M. G. Lattes, Science 107, 270 (1948)

2. H. Bradner, UCRL-486 (to be published)

3. E. McMillan and J. M. Peterson, Science 109, 438(A) (1949)

4. W. H. Barkas, A. S. Bishop, E. Gardner, C. M. G. Lattes, F. M. Smith (to be published)

5. M. Conversi, E. Pancini, O. Piccioni, Phys. Rev. 71, 209 (1947)

6. H. Bradner, UCRL-486 (to be published)

7. J. R. Richardson, Phys. Rev. 74, 1720 (1948)

8. E. Martinelli and W. K. H. Panofsky (to be published)

9. C. M. G. Lattes, G. P. S. Occhialini, C. F. Powell, Nature 160, 453, 486 (1947)

10. C. Richman and H. A. Wilcox (to be published)

11. V. Z. Peterson (private communication)

12. G. Wentzel, Phys. Rev. 75, 1810 (1949)

II-1. V. Z. Peterson, Phys. Rev. 75, 1469(A) (1948)

III-1. R. Bjorkland, W. Crandall, B. J. Moyer, H. York (to be published)

2. E. Gardner and F. M. Smith (private communication)

3. C. M. G. Lattes, G. P. S. Occhialini, C. F. Powell, Nature 160, 453, 486 (1947)

4. F. L. Adelman and S. B. Jones, Phys. Rev. 75, 1468(A) (1949)

5. W. Y. Chang, Rev. of Mod. Phys. 21, 166 (1949)

6. H. Bradner, UCRL-486 (to be published)

7. R. S. White and S. B. Jones (private communication)

V-1. J. R. Richardson, Phys. Rev. 74, 1720 (1948)

2. E. Martinelli and W. K. H. Panofsky (to be published)

3. R. S. White and S. B. Jones (to be published)

4. K. Brueckner (private communication)

VI-1. W. A. Aron, B. G. Hoffman, F. C. Williams, Collection of Range-Energy Curves, UCRL-121 Revised.

2. W. H. Barkas, A. S. Bishop, E. Gardner, C. M. G. Lattes, F. M. Smith (to be published)

3. W. H. Barkas, A. S. Bishop, H. Bradner, F. M. Smith, Phys. Rev. (in print)

4. C. Richman and H. A. Wilcox (to be published)

5. T. B. Taylor and G. F. Chew, Bul. Am. Phys. Soc. 24, 9 (1949)

6. G. F. Chew and J. L. Steinberger, Bul. Am. Phys. Soc. 24, 9 (1949)

VII-1. G. Wentzel, Phys. Rev. 75, 1810 (1949)